ELSEVIER

Journal of Nuclear Materials 302 (2002) 165–174

journal of nuclear materials

www.elsevier.com/locate/jnucmat

Ab initio study on the mechanism of hydrogen release from the silicate surface in the presence of water molecule

T. Nakazawa [a,*], K. Yokoyama [a], V. Grismanovs [b], Y. Katano [c], S. Jitsukawa [a]

[a] *Japan Atomic Energy Research Institute, Tokai-mura, Naka-gun, Ibaraki-ken 319-1195, Japan*
[b] *OECD Halden Reactor Project, P.O. Box 173, N-1751 Halden, Norway.*
[c] *Nippon Advanced Technology Co., Ltd., Tokai-mura, Naka-gun, Ibaraki-ken 319-1112, Japan*

Received 10 September 2001; accepted 19 January 2002

Abstract

The mechanism of the reaction of a water molecule with surface isolated hydroxyl of silica and silicates is investigated by ab initio molecular orbital calculations within a model reaction, $H_2O + H_3SiOH$, to figure out the role of water molecules in tritium release process. The hydrogen release from the surface isolated hydroxyl is found to proceed as a result of the Si–O bond breaking. Namely, tritium would be released by the hydroxyl-exchange reaction between water and surface hydroxyl of silicate, not by the hydrogen-exchange reaction. Prior to the exchange reaction, water molecules are found to prefer adsorbing as proton acceptors in the water – silanol complex, whereas the hydroxyl-exchange reaction occurs from a complex with a different form, in which the water molecule adsorbs as a proton donor. The overall potential energy barrier is calculated as 24.4 kcal mol^{-1} for the hydrogen release from the silicate in the presence of water molecules.

PACS: 82.65.M; 31.15.A; 71.15.F; 68.35.B

1. Introduction

Silica and silicates are widely used materials in various technologies: in applications ranging from nuclear energy through applied chemistry to biological systems. In the nuclear technology, silicate compounds containing lithium are among candidates as solid breeder materials. The release behavior of tritium generated by the $^6Li(n,\alpha)^3H$ reactions in those materials is considered as one of important problems to be thoroughly studied [1,2]. Additions of various gases, e.g. H_2, H_2O, C_2H_4, etc., to the sweep gas are often adopted for enhancing tritium release [3–5]. However, the mechanism of reaction between the tritium existed as surface hydroxyl and the added gases was poorly explored. In the applied chemistry such as oil industry, the surface properties of amorphous silica and silicates are the most extensively studied subjects, because of the importance of such material in adsorption and catalysis [6,7]. In biological research of inhaled silica particles [8], the silica surface sites readily reacting with both O_2 and H_2O are regarded as possible initiators of the macrophage-mediated reaction resulting in the lung fibrosis. Thus, descriptions of microscopic mechanisms for adsorption and reaction at the surfaces of silica and silicate are fundamentally important for various systems.

A large number of theoretical [6,9,10] and experimental [11–13] studies have been reported for gas-phase adsorption phenomena and adsorptive interactions between adsorbates and the surface of silica and silicates. Microscopic information has been obtained about the adsorption phenomena on the silica and silicate surfaces, such as adsorptive interaction energies and adsorption structures and their relations. However, the mechanism

* Corresponding author. Tel.: +81-29 282 6553; fax: +81-29 282 6556.
E-mail address: naka@maico.tokai.jaeri.go.jp (T. Nakazawa).

0022-3115/02/$ - see front matter
PII: S0022-3115(02)00779-1

of reactions of adsorbed molecules at the silica and silicate surfaces has not yet been studied systematically.

Recently, we have investigated the influence of trivalent elements, such as B, Al and Ga, on the properties of surface hydroxyls in lithium silicate [14,15] and the effects of the Al atom on the formation and desorption reactions of H_2O molecules from surface hydroxyl groups in silicates by ab initio molecular orbital calculations [16].

In the present study, we discuss the mechanism for the reaction of a water molecule with surface isolated hydroxyl of silica and silicates. Previous studies [9] have shown that the silanol molecule (H_3SiOH) can act as a suitable model for isolated hydroxyl groups of gels, glasses, polymers and crystals of silica and silicates. Therefore, in this study an H_3SiOH molecule is used to investigate weak interaction and hydrogen release process resulting from exchange reaction of water molecule with a hydroxyl group in silicates. We have carried out ab initio molecular orbital calculations to investigate the exchange reaction paths between H_2O and H_3SiOH molecules.

2. Method

To investigate the hydrogen release due to exchange reaction between water and surface hydroxyl of silicates, we have used the method of computational quantum chemistry to determine the minimum energy geometries of adsorption complexes and the transition structures in the reaction. Silanol (H_3SiOH) is chosen as the simplest molecular model of the surface isolated hydroxyl of silicate. This simplest molecular model has been used in previous works to represent the free hydroxyl of silicate.

All calculations have been performed at ab initio level with the GAUSSIAN98 program [17]. Basis sets adopted are 3-21G and 6-31G**. The 3-21G basis set is a small split-valence basis set, while the 6-31G** basis set is a larger split-valence basis set which includes p- and d-type polarization functions for the hydrogen and heavy atoms, respectively. Full geometry optimization has been carried out at the Hartree–Fock (HF) level with these basis sets for all structures by analytical gradient techniques. The geometry optimizations have been also done using Møller–Plesset second-order perturbation theory (MP2), which accounts for electron correlation. No symmetry constraints have been assumed in the geometry optimization. In each case, the vibrational frequencies have been calculated using analytical second derivatives of the total energy to ensure that the stationary points have been local minima of the potential energy surface. The transition states (TS) reported here have been confirmed to have one imaginary frequency. The unscaled frequencies have been used in the calculations for the correction of the vibrational zero-point energy (ZPE). Atomic charges on each atom in molecular models have been obtained from a Mulliken population analysis [18]. The intrinsic reaction coordinates (IRC) have been calculated in order to check and obtain energy profiles of the proposed reactions. Total energy (E_t) is calculated as the sum of the electronic energy (E_e) and the ZPE (E_{ZPE}) for each step in the reaction. The relative energy is the difference between the sum of the total energies of the H_2O and H_3SiOH molecules and the total energy of each step in the reactions. Interaction energy (E_{int}) is calculated as a difference of the sum of the electronic energies of the H_2O and H_3SiOH molecules and the electronic energies of the adsorption complex.

3. Results and discussions

3.1. Polarization function and electron correlation effects

3.1.1. H_3SiOH and H_2O molecules

The structures of H_3SiOH and H_2O molecules are illustrated in Fig. 1(I) and (II), respectively. The optimized geometrical parameters, atomic charges and total

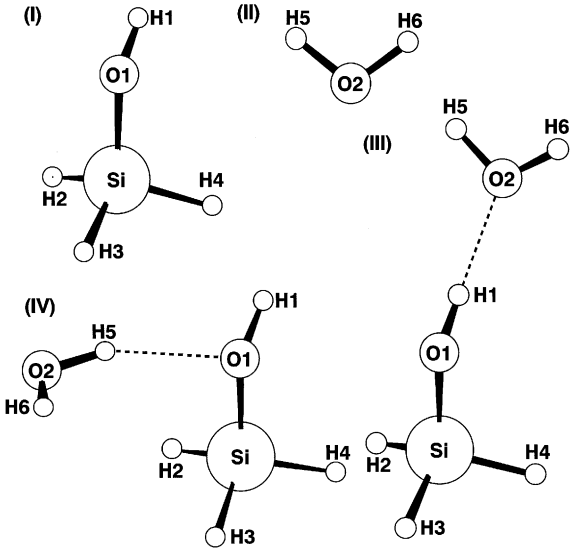

Fig. 1. Optimized structures of free silanol and water molecules and of two types of the $H_3SiOH\cdots H_2O$ complexes: (I) free silanol molecule, H_3SiOH; (II) water molecule, H_2O; (III) silanol with adsorbed H_2O molecule forming a proton acceptor hydrogen bond; (IV) silanol with adsorbed H_2O molecule forming a proton donor hydrogen bond. The geometrical parameters for free silanol and water molecules are in Table 1. The geometrical parameters for the adsorption complex (III) are in Table 2. The geometrical parameters for the adsorption complex (IV) are in Table 3.

Table 1
Geometrical parameters, atomic charges, bond overlap populations and energies for H_3SiOH and H_2O

	HF/3-21G	HF/6-31G**	MP2/6-31G**
(I) H_3SiOH			
Parameters			
Si–O1	1.675	1.644	1.669
O1–H1	0.960	0.941	0.961
Si–H2	1.488	1.478	1.478
Si–H3	1.477	1.470	1.468
Si–H4	1.488	1.478	1.478
∠Si–Ol–H1	126.84	120.01	116.68
∠Ol–Si–H2	112.20	111.42	112.13
∠Ol–Si–H3	106.99	106.91	105.85
∠O1–Si–H4	112.20	111.42	112.13
τ[H2–Si–O–H1]	−60.43	−60.16	−60.52
τ[H3–Si–O–H1]	180.03	180.00	180.02
τ[H4–Si–O–H1]	60.48	60.17	60.52
Atomic charges			
q(Si)	1.179	0.988	0.988
q(O1)	−0.877	−0.754	−0.764
q(Hl)	0.411	0.353	0.355
q(H2)	−0.247	−0.203	−0.200
q(H3)	−0.220	−0.181	−0.179
q(H4)	−0.247	−0.203	−0.200
Bond overlap populations			
n(Si–O1)	0.294	0.338	0.331
n(O1–H1)	0.270	0.322	0.313
Energies			
E_e	−364.180602	−366.141921	−366.426774
E_{ZPE}	0.040109	0.041305	0.040001
E_t	−364.140493	−366.100615	−366.386773
(II) H_2O			
Parameters			
O2–H5,6	0.967	0.943	0.961
∠H5–O2–H6	107.70	105.90	103.81
Atomic charges			
q(O2)	−0.733	−0.671	−0.674
q(H5,6)	0.366	0.335	0.337
Bond overlap populations			
n(O2–H5,6)	0.264	0.314	0.307
Energies			
E_e	−75.585960	−76.023615	−76.219786
E_{ZPE}	0.021775	0.023201	0.021880
E_t	−75.564184	−76.000414	−76.197905

Bond lengths (X–Y) in Å, bond angles (∠XYZ) and dihedral angle (τ[WXYZ]) in degrees and electronic energies (E_e), zero point ones (E_{ZPE}) and total ones (E_t) in hartrees. W, X, Y and Z refer to atoms as in Fig. 1.

energies are given in Table 1 at HF/3-21G, HF/6-31G** and MP2/6-31G** levels. Silanol (H_3SiOH) is unstable and cannot be isolated due to its rapid intermolecular condensation to siloxane ($H_3SiOSiH_3$) [19], therefore an experimental information on the structure is lacking. Some previous studies [9,20,21] have presented the minimum-energy static structures of H_3SiOH which were obtained with the optimization under the constraint of C_s symmetry. The geometrical parameters calculated for H_3SiOH molecule show that the symmetry of structure optimized in this study is very close to the C_s symmetry. Comparison with the literature data

[9,20,21] shows a good agreement with our results at the same level of calculation.

For the H_3SiOH and H_2O molecules the geometrical parameters, atomic charges and total energies vary significantly with the basis set size and electron correlation (see Table 1).

Addition of polarization functions decreases the Si–O1 and O1–H1 bond lengths in the H_3SiOH molecule, while inclusion of the electron correlation increase these bond lengths. Same tendencies are observed for the O–H bond distances in the H_2O molecule. The absolute magnitudes of atomic charges are reduced by the addition of polarization functions. The inclusion of electron correlation little influences the atomic charges. Total energies of H_3SiOH and H_2O molecules are reduced with the polarization function and the electron correlation effects.

The addition of polarization functions in general has the effect of increasing electron density in bonding regions (increasing overlap), which tends to reduce the bond lengths and the atomic charges [22]. While, the inclusion of electron correlation has the effect of redistribution in electron density away from bond center toward the exterior of molecules, which tends to extend the bond length [23]. The minor affect on the calculated charges is caused by the redistribution in electron density due to the electron correlation [22]. Moreover, the exact description of electronic state given by these effects leads to the relatively small values for total energies.

These effects are also reflected in the calculated bond angles. The calculated bond angles exhibit a great sensitivity to the addition of polarization functions and the inclusion of electron correlation. The Si–O1–H1 bond angle is significantly decreased from 126.84° to 116.68° with the quality of theory. The H5–O2–H6 bond angle is decreased from 107.70° to 103.81° as well.

The changes of bond angles are related to the redistribution of electron density in bonding region. For oxygen-containing compounds, where hybridization of the s and p orbitals is likely, the electronegativity of the hybrid orbitals depends on the percentage of s and p character, and also on the bond angle [24,25]. The larger the bond angle, the more pronounced the s character and a higher electronegativity of the hybrid orbital to be expected. The electronegativity is changed with the redistribution of electron density in bonding region due to the polarization functions and the electron correlation effects as well as the percentage of s and p character [26]. Thus, the decreases in the bond angles are caused by both the electronegativity due to the polarization functions and the electron correlation effects.

3.1.2. Adsorption complexes

In general, the interaction of a H_2O molecule and a SiOH group can be of two types: one in which H_2O acts as a proton acceptor in a hydrogen bond to the hydrogen (structure III), or the other in which H_2O acts as a proton donor in a hydrogen bond to the oxygen (structure IV). The structures of two adsorption complexes are illustrated in Fig. 1. The optimized geometrical parameters, the atomic charges, and the total and interaction energies calculated for the adsorption complexes (III) and (IV) are given in Tables 2 and 3, respectively, at HF/3-21G, HF/6-31G** and MP2/6-31G** levels. The values of these data obtained for the adsorption complexes vary significantly with the addition of polarization functions and inclusion of electron correlation as well as for H_3SiOH and H_2O molecules (see Tables 2 and 3).

Changes observed in the intramolecular parameters of the adsorption complexes are similar to those observed for the H_3SiOH and H_2O molecules. The intramolecular bond lengths of the adsorption complexes are decreased with the addition of polarization functions, while they are increased with the inclusion of electronic correlation. The intramolecular bond angles of the adsorption complexes are decreased with the addition of polarization function, and are further decreased with the inclusion of electron correlation. Additionally, these effects affect the atomic charges and the total energies of adsorptions, the same as in the case of the H_3SiOH and H_2O molecules.

These changes observed for the adsorption complexes are similarly explained by the discussion in Section 3.1.1 on the effects of polarization function and electron correlation for H_3SiOH and H_2O molecules.

Intermolecular bond distances and interaction energies are also affected by the addition of polarization function and inclusion of electron correlation. These effects on the intermolecular parameters bond distances and interaction energies of adsorption complexes are different from those of the intramolecular parameters of H_3SiOH and H_2O molecules.

The intermolecular $O2\cdots H1$ distance of the adsorption complex (III) increases by the polarization effect: 1.710 Å (HF/3-21G), 1.945 Å (HF/6-31G**). The intermolecular $O1\cdots H5$ distance of the adsorption complex (IV) also increases by the above effect: 1.821 Å (HF/3-21G), 2.088 Å (HF/6-31G**). In contrast to the polarization effect, these intermolecular distances decrease by the electron correlation effect.

On the other hand, the intermolecular interaction energies, E_{int}, obtained for the complex (III) at the different theoretical level are 13.6 (HF/3-21G), 7.2 (HF/6-31G**) and 8.9 kcal mol^{-1} (MP2/6-31G**). The E_{int} energies for the complex (IV) at the different theoretical level, are 12.6 (HF/3-21G), 4.7 (HF/6-31G**) and 6.9 kcal mol^{-1} (MP2/6-31G**).

The electron correlation effect is a contrast to the polarization one in both the intermolecular distances and interaction energies. The intermolecular distances and interaction energies decrease with the polarization

Table 2
Geometrical parameters, atomic charges, bond overlap populations and energies for adsorption complexes (III)

	HF/3-21G	HF/6-31G**	MP2/6-31G**
Intermolecular parameters			
H1–O2	1.710	1.945	1.844
∠H1–O2–H5	115.64	117.01	108.70
∠O1–H1–O2	178.65	176.46	178.30
τ[O2–H1–O1–Si]	−179.07	0.00	180.00
Intramolecular parameters			
Si–O1	1.657	1.634	1.657
O1–H1	0.975	0.949	0.973
Si–H2	1.493	1.481	1.480
Si–H3	1.482	1.473	1.472
Si–H4	1.493	1.481	1.480
O2–H5	0.966	0.944	0.963
O2–H6	0.966	0.944	0.963
∠Si–O1–H1	128.22	119.10	116.11
∠Ol–Si–H2	113.22	112.15	112.84
∠O1–Si–H3	108.26	107.56	106.79
∠O1–Si–H4	113.22	112.15	112.84
∠H5–O2–H6	109.49	106.81	104.74
τ[H2–Si–O1–H1]	−60.62	−60.40	−60.69
τ[H3–Si–O1–H1]	180.00	180.02	180.00
τ[H4–Si–Ol–Hl]	60.62	60.40	60.69
Atomic charges			
q(Si)	1.184	0.990	0.990
q(O1)	−0.945	−0.793	−0.816
q(H1)	0.452	0.396	0.404
q(H2)	−0.263	−0.214	−0.211
q(H3)	−0.239	−0.194	−0.193
q(H4)	−0.263	−0.214	−0.211
q(O2)	−0.730	−0.677	−0.680
q(H5)	0.402	0.353	0.359
q(H6)	0.402	0.353	0.359
Bond overlap populations			
n(Si–O1)	0.316	0.354	0.348
n(O1–H1)	0.238	0.314	0.300
n(O2–H5)	0.264	0.315	0.307
n(O2–H6)	0.264	0.315	0.307
Energies			
E_e	−439.788211	−442.176512	−442.660736
E_{ZPE}	0.066032	0.067430	0.065040
E_t	−439.722179	−442.109082	−442.595696
E_{int}	−13.6	−7.2	−8.9

Bond lengths (X–Y) in Å, bond angles (∠XYZ) and dihedral angle (τ[WXYZ]) in degrees, electronic energies (E_e), zero point ones (E_{ZPE}) and total ones (E_t) in hartrees and interaction energies (E_{int}) in kcal mol^{-1}. W, X, Y and Z refer to atoms as in Fig. 1.

effect, while they increase with the inclusion of electron correlation.

Small basis sets, such as the 3-21G basis set, often lead to too-small intermolecular distances [27]. This is also reflected in the calculated interaction energies, which are decreasing with basis set expansion. The large basis sets including the polarization function allow a good description of electron density in the binding region of hydrogen-bonded complexes [10,28].

The contributions to the interaction energy in the hydrogen bonding are basically due to dispersive interaction, electrostatic interaction and electron transfer [28]. It has been found that the dispersion energy becomes more important for the hydrogen-bonded complexes and is sometimes even comparable to the Coulombic energy [28].

However, at HF level dispersion effects are neglected and independent basis set is used. Thus, quantitatively

Table 3
Geometrical parameters, atomic charges, bond overlap populations and energies for adsorption complex (IV)

	HF/3-21G	HF/6-31G**	MP2/6-31G**
Intermolecular parameters			
O1–H5	1.821	2.088	1.995
∠Si–O1–H5	96.96	106.62	101.08
∠O1–H5–O2	135.64	155.13	150.40
τ[O2–H5–O1–Si]	8.13	−3.61	1.20
Intramolecular parameters			
Si–O1	1.699	1.657	1.685
O1–H1	0.961	0.943	0.963
Si–H2	1.473	1.473	1.472
Si–H3	1.474	1.468	1.466
Si–H4	1.496	1.478	1.477
O2–H5	0.974	0.946	0.967
O2–H6	0.966	0.943	0.962
∠Si–O1–H1	123.58	119.03	115.96
∠O1–Si–H2	112.95	111.46	112.37
∠O1–Si–H3	110.58	106.63	105.76
∠O1–Si–H4	106.11	109.94	109.81
∠H5–O2–H6	108.59	105.87	103.63
τ[H2–Si–O1–H1]	−104.65	−68.13	−66.74
τ[H3–Si–O1–H1]	128.38	171.19	172.05
τ[H4–Si–O1–H1]	12.58	52.04	53.72
Atomic charges			
q(Si)	1.170	0.991	0.992
q(O1)	−0.899	−0.783	−0.799
q(H1)	0.416	0.360	0.363
q(H2)	−0.220	−0.186	−0.180
q(H3)	−0.235	−0.179	−0.179
q(H4)	−0.261	−0.199	−0.197
q(O2)	−0.759	−0.699	−0.702
q(H5)	0.422	0.366	0.372
q(H6)	0.365	0.329	0.331
Bond overlap populations			
n(Si–O1)	0.244	0.305	0.292
n(O1–H1)	0.269	0.321	0.313
n(O2–H5)	0.236	0.307	0.297
n(O2–H6)	0.260	0.313	0.305
Energies			
E_e	−439.786644	−442.172986	−442.657560
E_{ZPE}	0.067135	0.067560	0.065259
E_t	−439.719509	−442.105426	−442.592301
E_{int}	−12.6	−4.7	−6.9

Bond lengths (X–Y) in Å, bond angles (∠XYZ) and dihedral angle (τ[WXYZ]) in degrees, electronic energies (E_e), zero-point ones (E_{ZPE}) and total ones (E_t) in hartrees and interaction energy (E_{int}) in kcal mol^{-1}. W, X, Y and Z refer to atoms as in Fig. 1.

accurate binding energies cannot be expected. To account for dispersion effects, it is necessary to go beyond the HF level of theory and include electron correlation. Thus, the increase in interaction energies due to the electron correlation effect result from the better description of the electronic density and taking into account the dispersive interaction. The increase in the interaction energies lead to short intermolecular distances.

3.2. Hydrogen release reaction

Fig. 2 shows three feasible reaction paths, which lead to hydrogen and/or hydroxyl exchange reactions in adsorption complexes. The MP2/6-31G** relative energy profiles for paths A–C, shown in Fig. 2, are depicted in Fig. 3. It can be seen in Fig. 3 that the H_2O adsorbed as a proton acceptor is more stable than the H_2O adsorbed as a proton donor.

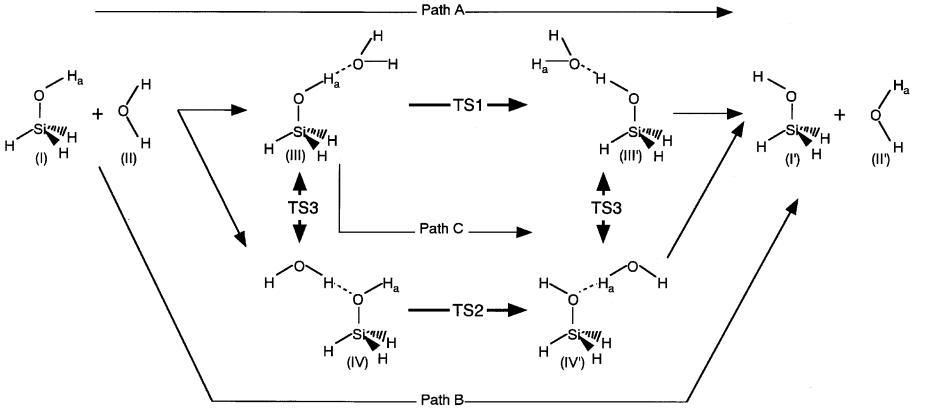

Fig. 2. Hydrogen release reaction paths between H_2O and H_3SiOH molecules.

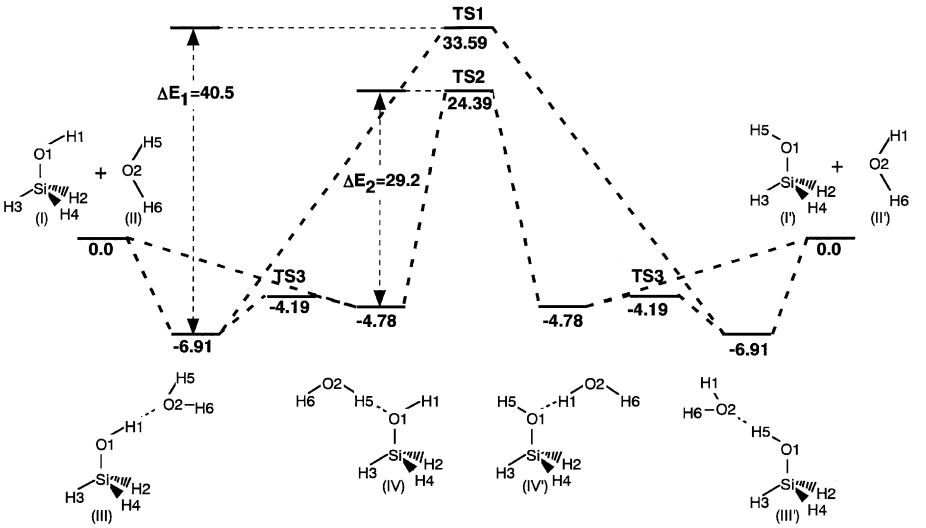

Fig. 3. MP2/6-31G** energy profiles (kcal mol^{-1}) of hydrogen release caused by exchange reactions between H_2O and H_3SiOH molecules. TS indicates the transition state (see text). The values in the figure are the relative energies. $\Delta E_{1,2}$ are the potential energy barriers for the exchange reactions.

The formation of structures (III) and (IV) at MP2/6-31G** level of theory is found to be exothermic by -6.91 and -4.78 kcal mol^{-1}, respectively, indicating that structure (III) is more stable than the structure (IV) on the silicate surface. In fact, the structure (III) has been found by an experimental technique to be the preferred one at the silicate surface [29,30].

When H_2O molecule adsorbs to the SiOH group as a proton acceptor to form the adsorption complex (III), the O1–H1 bond distance lengthens slightly and the Si–O1 bond distance is reduced. And also, the adsorption of H_2O as the proton acceptor increases the overlap population of the O1–H1 bond and decreases that of the Si–O1 bond, where the overlap population is calculated by the Mulliken population analysis and is considered to correspond to the bond strength [18]. These changes of bond distances and overlap populations indicate that the adsorption of H_2O as the proton acceptor makes the O1–H1 bond weak and the Si–O1 bond strong.

The interaction of H_2O as a proton donor affects the geometry and the charge distribution as well as when H_2O acts as a proton acceptor. When H_2O molecule adsorbs as a proton donor to the SiOH group to form the adsorption complex (IV), the distances of the O2–H5 bond and the Si–O1 bond lengthens slightly. Moreover, the adsorption of H_2O as the proton donor decreases the overlap populations of the O2–H5 bond and the Si–O1 bond. It is indicated from the decrease in the overlap

populations that both the O2–H5 and Si–O1 bonds are weakened by the adsorption of H_2O molecule as the proton donor.

As described above, the adsorption complex (III) differs from the adsorption complex (IV) in the changes of bond distances and overlap populations caused by the interaction of H_2O molecule with the SiOH group. These differences are associated with the difference in the mechanisms of the subsequent exchange reactions.

In the adsorption complex (III), the exchange of H atom takes place directly between the H_2O molecule and the SiOH group, because of the weakened O–H bond of the SiOH group due to the interaction of H_2O molecule as a proton acceptor. Fig. 4(a) shows the TS1 structure of the mechanism of the exchange reaction in the adsorption complex (III) and the hydrogen exchange reaction coordinate.

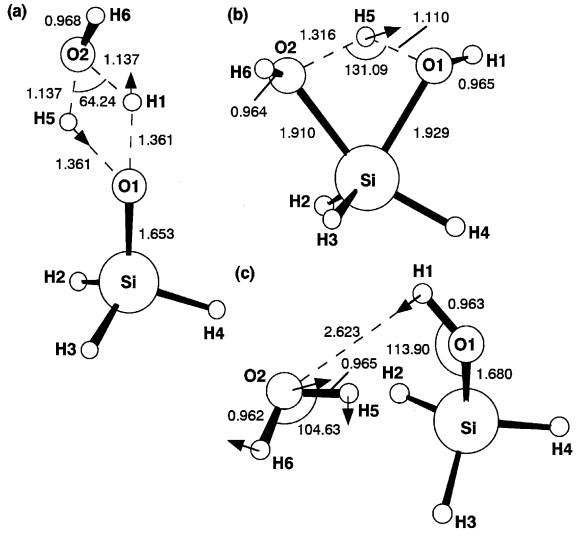

Fig. 4. MP2/6-31G** optimized structures for the transition state (a) TS1, (b) TS2 and (c) TS3. Bond lengths in Å, angles in degrees. HF/3-21G geometries: (a) Si–O1 = 1.652, O1–H1 = O1–H5 = 1.317, O2–H1 = O2–H5 = 1.154, O2–H6 = 0.964, ∠H1–O2–H5 = 66.00; (b) Si–O1 = 1.857, Si–O2 = 1.856, O1–H1 = 0.957, O1–H5 = 1.116, O2–H5 = 1.290, O2–H6 = 0.959, ∠O1–H5–O2 = 121.54; (c) Si–O1 = 1.686, O1–H1 = 0.962, O2–H5 = 0.967, O2–H6 = 0.966, O2–H1 = 2.548, ∠Si–O1–H1 = 121.93, ∠H5–O2–H6 = 109.14. HF/6-31G** geometries: (a) Si–O1 = 1.602, O1–H1 = O1–H5 = 1.514, O2–H1 = O2–H5 = 1.035, O2–H6 = 0.949, ∠H1–O2–H5 = 75.86; (b) Si–O1 = 1.864, Si–O2 = 1.918, O1–H1 = 0.944, O1–H5 = 1.101, O2–H5 = 1.283, O2–H6 = 0.943, ∠O1–H5–O2 = 130.62; (c) Si–O1 = 1.654, O1–H1 = 0.943, O2–H5 = 0.946, O2–H6 = 0.943, O2–H1 = 3.113, ∠Si–O1–H1 = 119.56, ∠H5–O2–H6 = 105.93. The arrows indicate the main components of the displacement vectors along the reaction coordinate.

On the other hand, a new water molecule is formed in the adsorption complex (IV) between the H atom of the adsorbed H_2O molecule and the –OH group in silanol because of the weakened Si–O bond due to the interaction of H_2O as proton donor. The remaining OH group in the water molecule bonds to the Si atom, and thus, a new hydroxyl is formed concertedly. Fig. 4(b) shows the TS2 structure of the mechanism of the exchange reaction in the adsorption complex (IV) and the hydroxyl exchange reaction coordinate. These rearrangements of bonds are confirmed to occur as a single elementary reaction by an IRC analysis.

Such difference in the mechanism of exchange reaction evidently gives different values for potential energy barriers calculated as a difference of the total energies of the transition state and the total energies of the adsorption complex (see Fig. 3). The potential energy barrier in the case of the adsorption complex (III) is estimated to be 40.5 kcal mol^{-1} at the MP2/6-31G** level, while that for the adsorption structure (IV) is estimated to be 29.2 kcal mol^{-1} at the same level of theory. The origin of such considerable difference in the potential energy barriers is thought to be due to the difference in strength of O–H and Si–O bonds. The O–H single bond energy has been experimentally obtained equal to 110.6 kcal mol^{-1} from literature [31], while the Si–O single bond energy has been experimentally obtained to be 88.2 kcal mol^{-1}.

As the adsorption complex (III) shifts to the TS1 state, remarkable change is observed for the O1–H1 bond length, which increases by approximately 40%. The increase in O1–H1 bond length requires the potential energy barrier of 40.5 kcal mol^{-1}, which is approximately 37% of the O–H single bond energy. On the other hand, with the shift from the adsorption complex (IV) to the TS2 state, slight change is observed for the Si–O1 bond length, which increases by about 14%. The increase in Si–O1 bond length causes the potential energy barrier of 29.2 kcal mol^{-1}, which is around 33% of the Si–O single bond energy. In the case of the exchange reaction in the adsorption complex (IV), the potential energy barrier, which corresponds to 33% of the Si–O single bond energy, results from 14% of increase for Si–O1 bond length. In the case of the exchange reaction in the adsorption complex (III), 40% of increase for O1–H1 bond length is required to cause the potential energy barrier corresponding to 37% of the O–H bond energy. These results suggest that the O1–H1 bond in the adsorption complex (III) is stronger than the Si–O1 bond in the adsorption complex (IV).

Three reaction paths can be considered as candidates for hydrogen release process due to exchange reactions between water and silanol molecule. The first is path A, that is water molecule adsorbs as a proton acceptor to the hydroxyl of silanol and exchange its own H atom for H atom in hydroxyl of silanol at TS1. The potential

energy barrier at the MP2/6-31G** level is calculated to be around 40.5 kcal mol^{-1} which is the energy between TS1 and (III) (see Fig. 3).

The second is path B, that is water molecule adsorbs as a proton donor to the hydroxyl of silanol and supplies its own H atom to the hydroxyl at the TS2 state to form a new water molecule. Simultaneously, the rest of water molecule bonds to Si atom to form a new hydroxyl, i.e. hydroxyl exchange reaction between water molecule and silanol. The potential energy barrier at the MP2/6-31G** level is estimated to be around 29.2 kcal mol^{-1} which is the energy between TS2 and (IV) (see Fig. 3). At the MP2/6-31G** level, the potential energy barrier for path B is smaller by 11.3 kcal mol^{-1} than that for path A. Thus, the path B is more favorable for the hydrogen release process than the path A. On the contrary, energetically favorable complex (III) is not the precursor of the hydroxyl exchange reaction, which is energetically favorable pathway for hydrogen release process, i.e. the path B. Therefore, the minimum-energy path of the hydrogen release should include the isomerization from (III) to (IV).

The energy level diagram shown in Fig. 3 presents another path C indicating such an isomerization process, which is calculated to be an endothermic reaction with an extremely small potential energy barrier around 2.7 kcal mol^{-1} at MP2/6-31G** level. After the isomerization, the hydroxyl-exchange reaction proceeds in the adsorption complex (IV) via TS2 and produces a new adsorption complex (IV′) which is identical with the adsorption complex (IV). The adsorption complex (IV′) is switched to the more stable complex (III′) with small energy via TS3. As a result, the minimum-energy path of the hydrogen release process is considered to be path C.

In this study, the overall potential energy barrier of the hydrogen release process is calculated as 24.4 kcal mol^{-1} with the rate-determining step in the hydroxyl-exchange reaction. Recently, we have reported that the energies for the H_2O formation and desorption reactions of the H_2O molecules from the geminal surafce hydroxyl in silicates were calculated to be 48.3 and 68.4 kcal mol^{-1} at the MP2/6-31G** level with the $Si(OH)_4$ cluster model [16]. These values are considerably larger than the overall potential energy barrier calculated here for the hydrogen release caused by the exchange reaction of H_2O molecule with H_3SiOH one. This indicates that the tritium release from lithium silicates as solid breeding material should be enhanced by the presence of water molecule in accordance with the experiment [5].

4. Conclusions

The hydrogen release reactions between water and silanol molecules have been investigated by the ab initio calculation. The minimum-energy path of the release reaction was concluded to consist of three steps. At the first step, the water molecule forms a hydrogen-bonded complex as a proton acceptor. At the second step, the water molecule changes its adsorption character from the proton acceptor to the proton donor by changing its adsorption site. At the third step, the hydrogen migration, the Si–O bond breaking, and a new Si–O bond formation proceed concertedly to form a new water molecule and silanol. The overall potential energy barrier is calculated as 24.4 kcal mol^{-1} for the hydrogen release process from silanol in the presence of water molecules.

Acknowledgements

We gratefully acknowledge the interest and encouragement presented from Dr A. Iwamoto.

References

[1] A. Abramenkovs, J. Tiliks, G. Kizane, V. Grishmanovs, A. Supe, J. Nucl. Mater. 248 (1997) 116.
[2] H. Kudo, K. Okuno, S. O'hira, J. Nucl. Mater. 155–157 (1988) 524.
[3] M. Matsuyama, T. Takeuchi, J. Nucl. Sci. Technol. 18 (1981) 15.
[4] D. Vollath, H. Wedemeyer, H. Zimmermann, H. Werle, J. Nucl. Mater. 174 (1990) 86.
[5] W. Breitung, H. Elbel, H. Wedemeyer, H. Werle, Fusion Technol. (1990) 886.
[6] T. Suzuki, M. Hirano, H. Tamon, M. Okazaki, J. Phys. Chem. 99 (1995) 15968.
[7] D.W. Breck, Zeolite Molecular Sieves, Wiley, New York, 1974.
[8] B. Fubini, V. Bolis, E. Giamello, Inorg. Chim. Acta 138 (1987) 193.
[9] B.C. Chakoumakos, G.V. Gibbs, J. Phys. Chem. 90 (1986) 996.
[10] J. Sauer, P. Ugliengo, E. Garrone, V.R. Saunders, Chem. Rev. 94 (1994) 2095.
[11] W. Hertl, M.L. Hair, J. Phys. Chem. 72 (1968) 4676.
[12] J. Shen, J.M. Smith, Ind. Eng. Chem. Fundam. 7 (1968) 100.
[13] R.W. Glass, R.A. Ross, Can. J. Chem. 50 (1972) 1241.
[14] T. Nakazawa, K. Yokoyama, K. Noda, J. Nucl. Mater. 258–263 (1998) 571.
[15] T. Nakazawa, K. Yokoyama, V. Grismanovs, Y. Katano, J. Nucl. Mater. 279 (2000) 201.
[16] T. Nakazawa, K. Yokoyama, V. Grismanovs, Y. Katano, J. Nucl. Mater. 297 (2001) 69.
[17] M.J. Frisch, G.W. Trucks, H.B. Schlegel, G.E. Scuseria, M.A. Robb, J.R. Cheeseman, V.G. Zakrzewski, J.A. Montgomery, R.E. Stratmann, J.C. Burant, S. Dapprich, J.M. Millam, A.D. Daniels, K.N. Kudin, M.C. Strain, O. Farkas, J. Tomasi, V. Barone, M. Cossi, R. Cammi, B. Mennucci, C. Pomelli, C. Adamo, S. Clifford, J. Ochterski,

G.A. Petersson, P.Y. Ayala, Q. Cui, K. Morokuma, D.K. Malick, A.D. Rabuck, K. Raghavachari, J.B. Foresman, J. Cioslowski, J.V. Ortiz, A.G. Baboul, B.B. Stefanov, G. Liu, A. Liashenko, P. Piskorz, I. Komaromi, R. Gomperts, R.L. Martin, D.J. Fox, T. Keith, M.A. Al-Laham, C.Y. Peng, A. Nanayakkara, C. Gonzalez, M. Challacombe, P.M.W. Gill, B. Johnson, W. Chen, M.W. Wong, J.L. Andres, C. Gonzalez, M. Head-Gordon, E.S. Replogle, J.A. Pople, Gaussian98, Revision A.7, Gaussian Inc., Pittsburgh, PA, 1998.

[18] R.S. Mulliken, J. Chem. Phys. 23 (1955) 1833.

[19] E.A.V. Ebsworth, Volatile Silicon Compounds, Pergamon, London, 1963;
F.W. Lampe, in: P. Ausloos (Ed.), Interaction Between Ions and Molecules, Plenum, New York, 1974.

[20] E. Garrone, V.B. Kazansky, L.M. Kustov, J. Sauer, I.N. Senchenya, P. Ugliengo, J. Phys. Chem. 96 (1992) 1040.

[21] P. Ugliengo, V.R. Saunders, E. Garrone, J. Phys. Chem. 93 (1989) 5210.

[22] C.W. Earley, J. Comput. Chem. 14 (1993) 216.

[23] K.B. Wiberg, C.M. Hadad, T.J. LePage, C.M. Breneman, M.J. Frisch, J. Phys. Chem. 96 (1992) 671.

[24] W.J. Mortier, J. Sauer, J.A. Lercher, H. Noller, J. Phys. Chem. 88 (1984) 905.

[25] I.N. Senchenya, V.B. Kazansky, S. Beran, J. Phys. Chem. 90 (1986) 4857.

[26] J. Hinze, H.H. Jaffe, J. Am. Chem. Soc. 84 (1962) 540.

[27] J. Limtrakul, J. Yoinuan, D. Tantanak, M.M. Probst, J. Mol. Struct. 312 (1994) 183.

[28] P. Hobza, R. Zahradnik, Chem. Rev. 88 (1988) 871.

[29] K. Klier, J. Chem. Phys. 58 (1973) 737.

[30] K. Klier, J.H. Shen, A.C. Zettlemoyer, J. Phys. Chem. 77 (1973) 1458.

[31] L. Pauling, The Nature of the Chemical Bond, Ithaca, NY, 1960.